Shaded-mask filtering: novel strategy for improvement of resolution in radial-polarization scanning microscopy

María Teresa Caballero
Universidad de Alicante
Departamento de Óptica
03080 Alicante, Spain

Cristina Ibáñez-López
Manuel Martínez-Corral, MEMBER SPIE
Universidad de Valencia
Departamento de Óptica
46100 Burjassot, Spain

Abstract. Radially polarized illumination produces, in combination with annular pupil filtering, the sharpest focal spot. However, the enhanced sidelobes produce an effective deterioration of spatial resolution. This study shows that if one substitutes the annular filter by one, adequately designed, shaded-mask filter, the sidelobes' strength is strongly reduced, and an important, effective improvement of resolution is achieved. [DOI: 10.1117/1.2345190]

Subject terms: resolution; scanning microscopy; apodization; diffractive optical elements; polarization.

Paper 050864R received Oct. 31, 2005; revised manuscript received Jan. 10, 2006; accepted for publication Jan. 13, 2006; published online Sep. 8, 2006.

1 Introduction

The improvement of the resolution of optical instruments and devices has been the aim of many research studies in the last few decades. As pointed out first by Abbe, after the formulation of his wave theory for microscopic imaging,[1] the spatial resolution is mainly restricted by the ability of imaging systems to produce a tight diffraction spot when imaging a light point source. One classic method suggested for obtaining a tighter diffraction spot is the insertion of an annular binary mask in the aperture stop.[2,3] This technique works fairly well in low numerical aperture (NA) imaging systems. However, when using modern microscope objectives with high NA, the polarization properties of the illumination light field play a dominant role.[4–8] This is because, in general, the three orthogonal field components appear in the focal region. As a result of it, the use of annular apertures does not produce the expected tighter focal spot, but a spot in which the longitudinal polarization component has increased its strength so that a pronounced asymmetry is induced. This is the focusing phenomenon known as the splitting effect.[9] As a result of it, the focal spot broadens and, consequently, the resolution worsens.

It has been recently demonstrated that annular filters can be still useful in high-NA focusing geometries provided that a special polarization pattern is used for the illumination. Specifically, Dorn et al.[10] experimentally demonstrated that radially polarized illumination produces a sharper focus, and it is immune to the splitting effect. So, annular filters can be used to make the focal spot even narrower. However, as we show in this paper, even in the case of working with such special illumination, the annular filters produce a strong detrimental effect if used in conventional wide field microscopes. We refer to the enhancement of the focal-spot sidelobes, which produce an effective deterioration of the lateral resolution.

What we propose in this paper is to use a modified version of the annular filters. We design a whole family of filters that are simply composed by a purely absorbing circular mask. We will see that by adequately changing the area and transmittance of the shaded mask, one can modify at will, between certain limits, the percentage of energy within the lateral sidelobes. We show that when one of these filters is inserted in the aperture stop of the focusing objective of a scanning microscope, an effective improvement of resolution is achieved.

The paper is organized as follows. In Sec. 2, we compare the focusing properties of linearly and radially polarized light beams. In Sec. 3, we study the utility of annular filters in systems under radially polarized illumination and conclude that even when working with such illumination, the use of the filter deteriorates the spatial resolution. In Sec. 4, we change the strategy and study the utility of pupil filtering in nonlinear scanning microscopy. To this end, we extend the paraxial concept of resolution gain to the case of strongly focused radially polarized fields. This new parameter allows us to design a novel class of pupil filters, the so-called shaded-mask (SM) filters. These filters have the ability of narrowing the focal spot but avoiding the enhancement of the sidelobes. We show that by inserting an adequately selected SM filter in the objective aperture stop, an important improvement of lateral resolution can be effectively achieved. Finally, in Sec. 5, we outline the main achievements of this work.

2 The Structure of Tightly Focused Radially Polarized Light Beams

Let us start by considering the case of a linearly polarized, monochromatic plane wave that impinges on a high-NA focusing system, as schematized in Fig. 1. According to the electromagnetic focusing theory of Richards and Wolf,[11] the electric-field distribution in the focal region is given by

$$\mathbf{E}(r,z,\varphi;\lambda) = [I_0(r,z;\lambda) + I_2(r,z;\lambda)\cos 2\varphi]\mathbf{i} + I_2(r,z;\lambda)\sin 2\varphi\mathbf{j} + i2I_1(r,z;\lambda)\cos \varphi\mathbf{k}, \quad (1)$$

where $I_{0,1,2}$ are integrals over the aperture angle θ. Param-

0091-3286/2006/$22.00 © 2006 SPIE

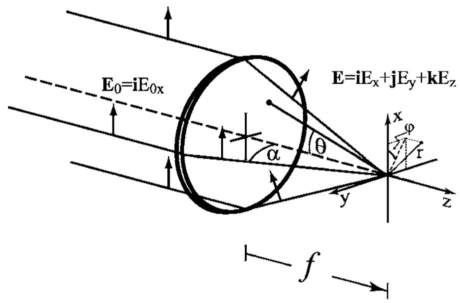

Fig. 1 Ray tracing model for the focusing of an *x*-polarized plane wave.

eter φ accounts for the angle between the polarization direction of the incident field (assumed, without loss of generality, to be x polarized) and the meridian plane under study. Note, from Eq. (1), that field components perpendicular to the initial polarization appear in the focal region. Besides, due to the explicit dependence with φ, the field components are not radially symmetric (see Fig. 2).

Strong focusing is the key for obtaining high resolution in imaging systems. Scanning microscopes constitute the most widely used technique in the area of three-dimensional (3D) micro imaging. To improve their lateral resolution, the use of annular masks has been classically proposed. However, as shown by Gu and coworkers,[9] when such devices work with high-NA focusing elements and linearly polarized illumination, the use of annular masks produce an undesired splitting effect in the focal spot. When this occurs, instead of the expected superresolution effect, an effective deterioration of lateral resolution is achieved.

A novel strategy for avoiding the detrimental consequences of the splitting effect was proposed by Dorn et al.[10] Their approach is based in the use of radially polarized illumination. It is straightforward to find that, under such illumination, the electric field in the focal region has only two polarization components. One is in the radial direction and the other in the longitudinal one. In mathematical terms,

$$\begin{aligned}\mathbf{E}(r,z,\varphi;\lambda) &= I_1'(r,z;\lambda)\cos\varphi\mathbf{i} + I_1'(r,z;\lambda)\sin\varphi\mathbf{j} \\ &\quad + 2iI_0'(r,z;\lambda)\mathbf{k} \\ &= I_1'(r,z;\lambda)\mathbf{g} + 2iI_0'(r,z;\lambda)\mathbf{k},\end{aligned} \tag{2}$$

where $\mathbf{g}=\cos\varphi\mathbf{i}+\sin\varphi\mathbf{j}$ represents the radial unit vector, and $I_{0,1}'$ are the following integrals,

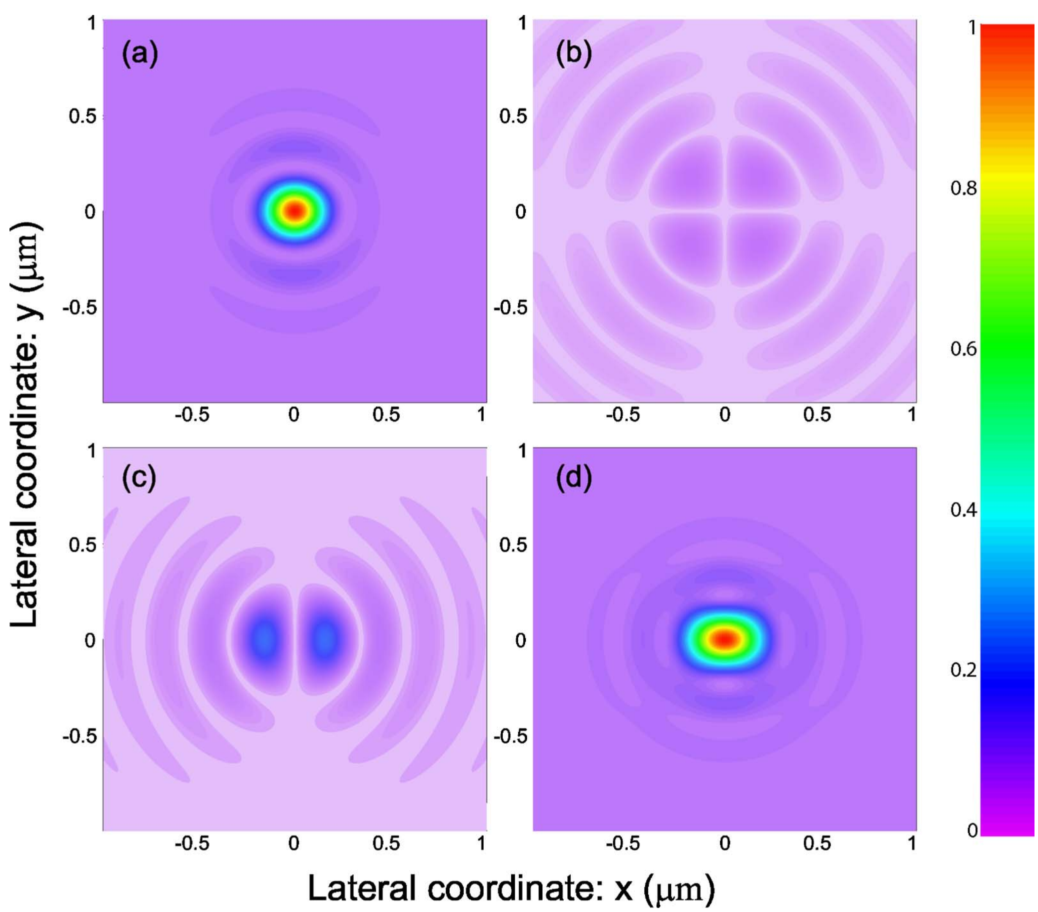

Fig. 2 Three-dimensional maps, for an objective with NA=1.4 (oil), *x*-polarized illumination, and a clear circular aperture, of the following normalized intensities: (a) $|E_x(r,z=0)|^2$, (b) $|E_y(r,z=0)|^2$, (c) $|E_z(r,z=0)|^2$, and (d) $|\mathbf{E}|^2=|E_x|^2+|E_y|^2+|E_z|^2$. In the calculations, we assumed that $\lambda=632.8$ nm.

$$I'_0 = \frac{\pi}{\lambda}\int_0^{\alpha} P(\theta) J_0(kr \sin\theta)\exp(-ikz\cos\theta)\sin^2\theta d\theta, \tag{3}$$

$$I'_1 = \frac{\pi}{\lambda}\int_0^{\alpha} P(\theta) J_1(kr \sin\theta)\exp(-ikz\cos\theta)\sin 2\theta d\theta, \tag{4}$$

where r and z are radial and axial coordinates, as measured from the focus of the wave front, $J_n(\bullet)$ is the nth-order Bessel function, and $P(\theta)$ is the pupil function.

Because we are interested in the transverse section of the focal field, we can particularize the previous equations to points in the focal plane, and obtain

$$\mathbf{E}(r,0;\lambda) = \frac{\pi}{\lambda}\left\{\int_0^{\alpha} P(\theta)[J_1(kr\sin\theta)\sin 2\theta\mathbf{g} + 2iJ_0(kr\sin\theta)\sin^2\theta\mathbf{k}]d\theta\right\}. \tag{5}$$

In Fig. 3, we have represented the normalized intensity distribution of the electric-field components in the focal plane. Note that in this case, most of energy (68%), is associated with the longitudinal component of the field. This percentage is much higher when an annular filter is inserted. For this reason, in such a case, one can accurately approximate the field in the focal plane by

$$\mathbf{E}(r,0;\lambda) \approx 2iI'_0(r,0;\lambda)\mathbf{k} = \frac{2i\pi}{\lambda}\int_0^{\alpha} P(\theta)J_0(kr\sin\theta)\sin^2\theta\, d\theta\,\mathbf{k}. \tag{6}$$

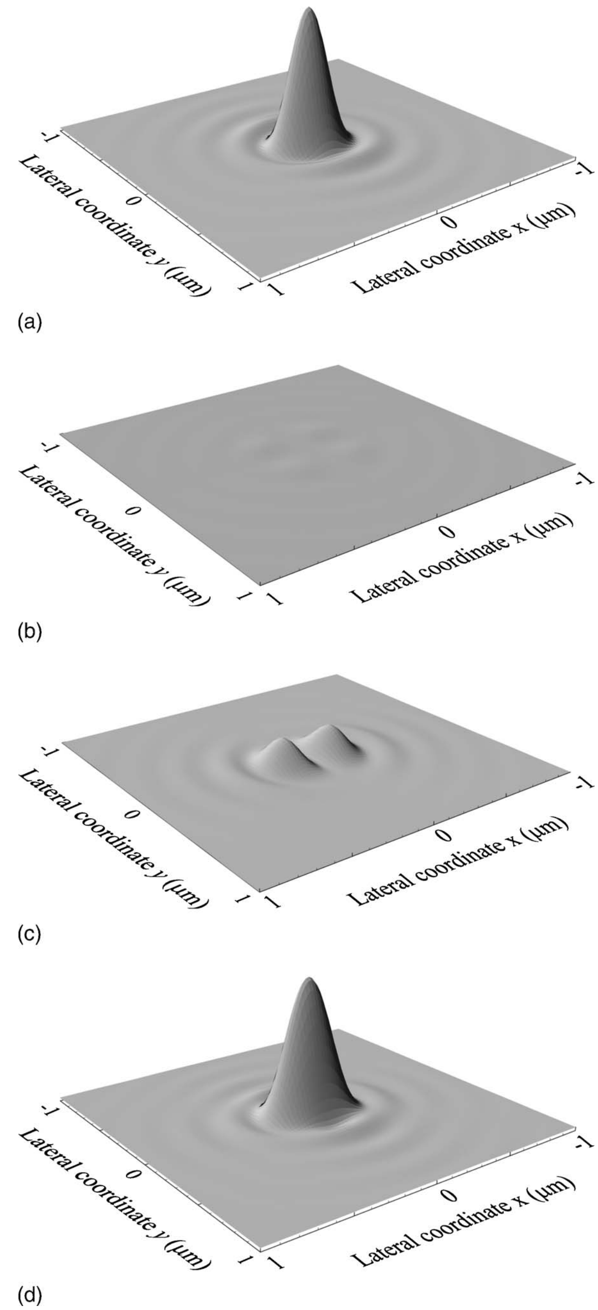

Fig. 3 Same three-dimensional maps as in Fig. 2, but for the case of radially polarized illumination. In this case, the overall intensity distribution is radially symmetric.

3 Lateral Resolution Improvement by Annular Filters

The insertion of an opaque circular mask centered in the aperture stop of a high-NA objective produces a significant narrowness of the central lobe of the focal spot provided that the objective is illuminated by a radially polarized light beam. To illustrate this fact, in Fig. 4, we have plotted the intensity distribution in the focal plane corresponding to the circular aperture and also to the annular filter. For these calculations, we have selected the annular pupil such that its light throughput is half the light throughput of the circular aperture. Note, however from the figure, that the important narrowness of the central lobe [14% in terms of the full width at the half maximum (FWHM)] is accompanied by a significant enhancement of the lateral sidelobes. So, it is not clear from the figure if the new focal spot really improves the lateral resolution. To respond to this question, it is convenient to calculate the Hankel transform of curves in Fig. 4, that is, the so-called optical transfer function (OTF). In Fig. 5, we have plotted the OTFs and found how detrimental the sidelobes' enhancement is. The inspection of this figure shows that the spatial-frequency transference obtained with the annular filter is much worse than the transference corresponding to the circular aperture over 84% of the frequency range. Thus, one can readily conclude that contrary to what is usually assumed, the annular binary mask does deteriorate the resolution of microscopes, even in the optimum case of radially polarized illumination.

A different question is the utility of pupil engineering in nonlinear scanning microscopy. Let us focus our attention in the two-photon excitation (TPE) scanning microscopy. This nonlinear imaging technique relies on the simultaneous absorption of two photons, whereby a single fluorescence photon is emitted.[12] The overall fluorescent light is collected and finally the image is synthesized from the 3D sampling of the object. TPE fluorescence microscopy can be considered as self-pinholed due to the square dependence of the up-converted signal with the incoming inten-

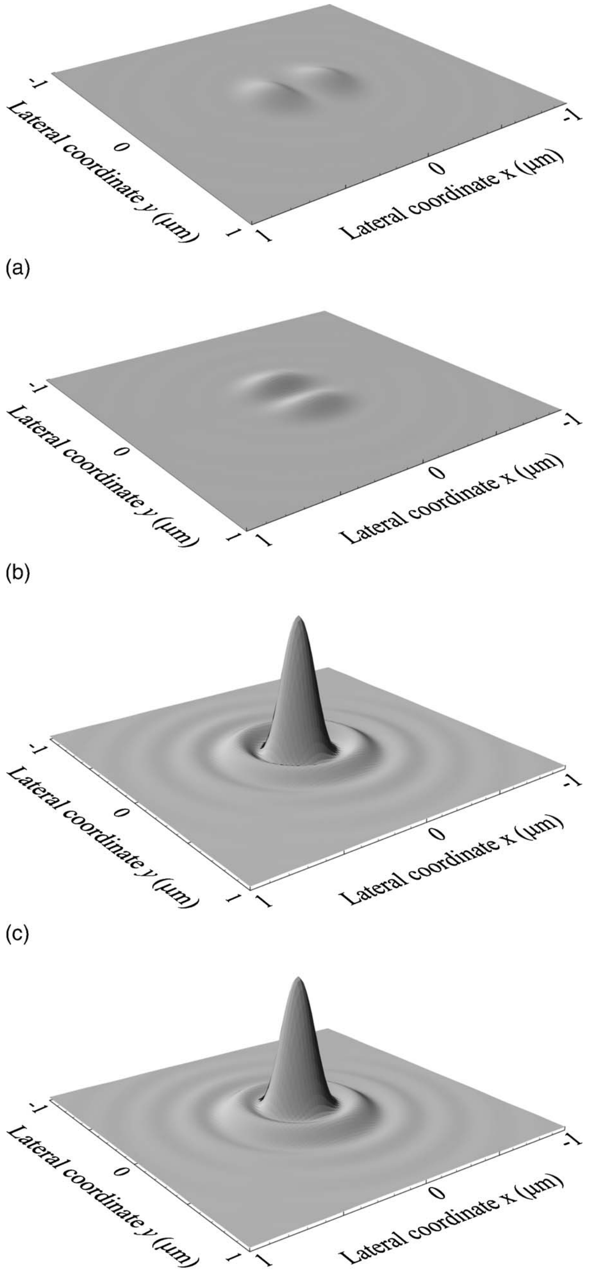

Fig. 4 Normalized intensity distribution in the focal plane under radially polarized illumination. For the calculation, performed according to Eq. (6), we considered NA=1.4 (oil) and λ=632.8 nm.

sity. As a result of that, contrast is dramatically enhanced by the subsequent sidelobes lowering in the illuminating spot. In Fig. 6, we have plotted the TPE point spread functions (PSFs) and OTFs corresponding to the unapodized circular aperture and the annular mask. The calculations of $|\mathbf{E}(r,0;\lambda)|^4$ were done according to Eq. (5). Note that now the annular binary mask produces small sidelobes, and consequently, the frequency transference is enhanced over a wide range of lateral frequencies, giving rise to an effective improvement of lateral resolution.

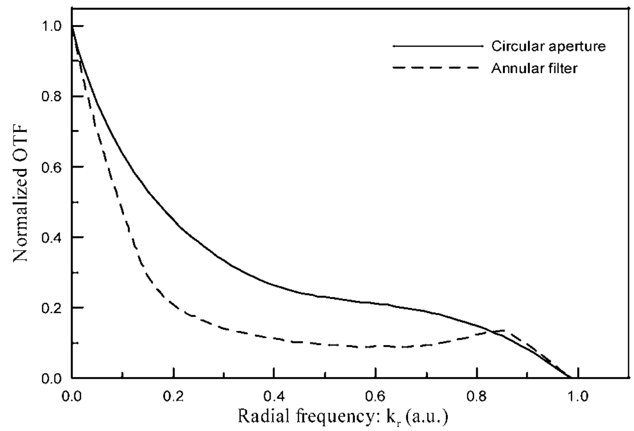

Fig. 5 Normalized OTFs.

4 The Design of SM Filters

A drawback that appears inherent to the use of annular masks in TPE scanning microscopy is photobleaching. Note that, although at any scanning position only a small region of the sample is imaged; the whole sample is slightly bleached due to the sidelobes height enhancement. To reduce this detrimental effect, we propose to apply the shaded-ring (SR) concept, which was designed to improve the optical sectioning capacity of scanning microscopes,[13] the lateral resolution. The design procedure is similar to that reported by Martinez-Corral et al.,[14] but adapted to the lateral response of high-NA focusing elements under radially polarized illumination. Then we first need to define a parameter that evaluates the narrowness produced, on the PSF, when using a pupil filter. Such a parameter was already defined in a paraxial context. We refer to the resolution gain parameter. So, what it is necessary at this point is to adapt the paraxial, scalar, concept of resolution gain to the more general case of strongly focused, radially polarized light beams. To this end, we first rewrite Eq. (6) as

$$\mathbf{E}(r,\theta;\lambda) = \mathbf{k}\frac{2\pi i}{\lambda}\int_{\cos\,\alpha}^{1} Q(\zeta)\sqrt{1-\zeta^2}J_0(kr\sqrt{1-\zeta^2})d\zeta, \tag{7}$$

where

$$\zeta = \cos\,\theta, \quad Q(\zeta) = P(\theta). \tag{8}$$

The lateral PSF of the TPE scanning microscope is given by

$$PSF_{2\mathrm{p}} = |\mathbf{E}(r,0;\lambda)|^4. \tag{9}$$

Next, we expand the normalized PSF into a power series, up to a second-order approximation and, after straightforward calculations, find that

$$PSF_{2\mathrm{p}}^{\mathrm{N}}(r) = \frac{PSF_{2\mathrm{p}}(r,0;\lambda)}{PSF_{2\mathrm{p}}(0,0;\lambda)} \approx 1 - \frac{k^2}{2}\left(1 - \frac{m_2}{m_0 - \frac{1}{2}m_2}\right)r^2, \tag{10}$$

where m_n is the nth-order moment of function $Q(\zeta)$, defined by

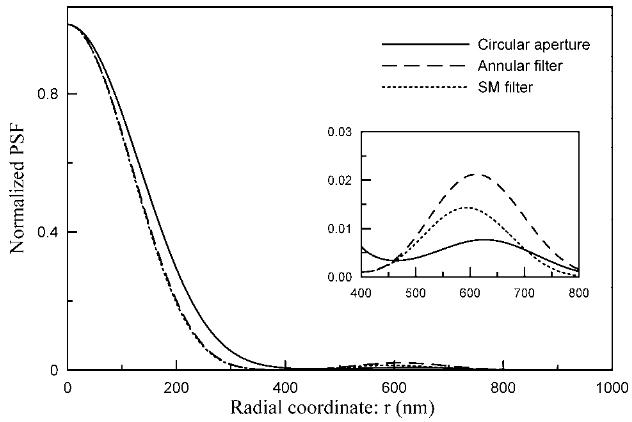

(a)

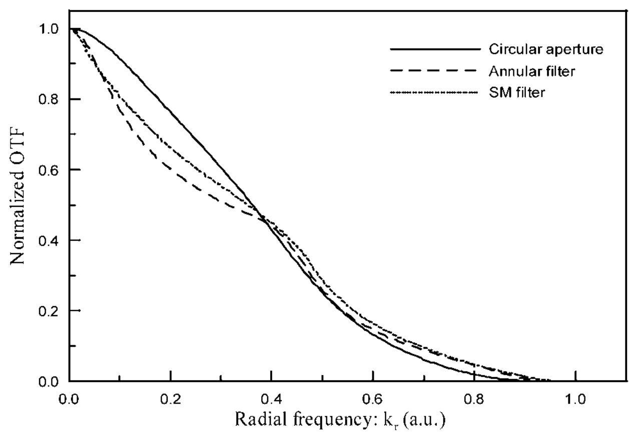

(b)

Fig. 6 (a) Normalized intensity distributions in the focal plane corresponding to the circular aperture (solid line), the annular aperture (dashed line), and the selected SM filter (dotted line). (b) The normalized OTFs.

$$m_n = \int_{\cos\alpha}^{1} Q(\zeta)\zeta^n d\zeta. \tag{11}$$

In the proposed second-order approximation, the normalized PSF is a parabolic function whose width is proportional to $(1-m_2/[m_0-m_2/2])^{-1/2}$. Given a pupil mask, one can define the gain in transverse resolution, G_T, as the ratio between the PSF width corresponding to the mask and the one of the circular aperture. Therefore,

$$G_T = \sqrt{\frac{\left(1-\dfrac{m_2}{m_0-\frac{1}{2}m_2}\right)_{\mathrm{c}}}{\left(1-\dfrac{m_2}{m_0-\frac{1}{2}m_2}\right)_{\mathrm{m}}}}, \tag{12}$$

where subscript m refers to the mask, and subscript c to the nonapodized circular pupil.

Our proposal here is to substitute the opaque circular mask by an adequate shaded circular mask. The actual form of the resulting SM filters, which can be understood as members of a more general class of filters known as leaky filters,[15] is shown in Fig. 7. The mapped transmittance is a function of two parameters, μ and η. Consequently, the

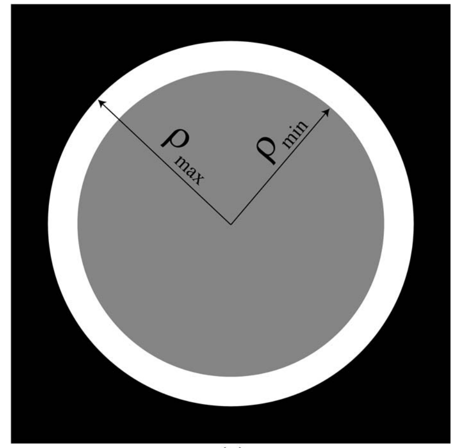

(a)

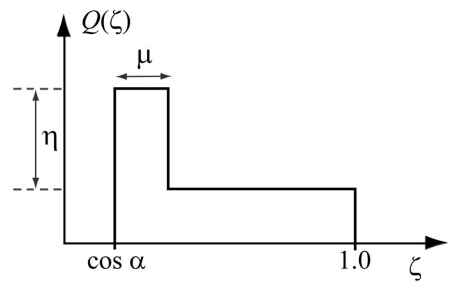

(b)

Fig. 7 (a) The SM filter is composed of a partially transmitting neutral circular mask centered in the circular aperture. (b) Mapped transmittance of the SM filter.

gain resolution depends on these parameters as well. Calculation of moments for the SM filters gives

$$m_{\mathrm{o,c}} = 1-\cos\alpha, \quad m_{2,\mathrm{c}} = \frac{1}{3}(1-\cos^3\alpha) \tag{13}$$

and

$$m_{\mathrm{o,m}} = (1-\eta)(1-\mu)+\mu-\cos\alpha,$$
$$m_{2,\mathrm{m}} = \frac{1}{3}[\mu^3+(1-\eta)(1-\mu^3)-\cos^3\alpha]. \tag{14}$$

Consequently, the transverse gain is

$$G_{\mathrm{T}} = \sqrt{\frac{3+\dfrac{12}{\cos^2\alpha+\cos\alpha-5}}{3-\dfrac{12(-1+\eta-\eta\mu+\cos\alpha)}{-\cos^3\alpha+6\cos\alpha+\eta(\mu^3-6\mu+5)-5}}}. \tag{15}$$

Note that, given a value for G_T, all pairs (η,μ) fulfilling Eq. (15) correspond to filters with the same central-lobe width, but different sidelobes energy. Any pair $(\eta=1, \mu)$ corresponds to an annular binary, considered now as a member of the SM-filters family.

According to our aim of minimizing the sidelobes' strength for a given value of G_T, we will select the leaky

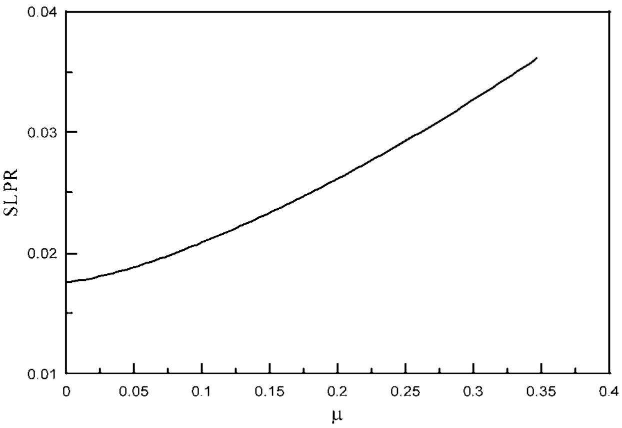

Fig. 8 SLPR values for the family of SM filters with the same resolution gain as the annular filter used in the previous calculations.

filter that maximizes the focused-light efficiency, understood as the ratio between the central-lobe energy and the overall diffracted energy. In other words, the one that minimizes the sidelobes to peak ratio (SLPR), defined as

$$SLPR = \int_{r}^{+\infty} |\mathbf{E}(r,0;\lambda)|^4 dr \Bigg/ \int_0^{r} |\mathbf{E}(r,0;\lambda)|^4 dr, \qquad (16)$$

with r_1 being the radial coordinate of the first minimum.

We have calculated the family of SM filters with the same resolution gain as the annular binary filter used in the previous calculations; that is, G_T=0.72. In Fig. 8, we have plotted the values of SLPR. As stated above, the binary filter appears the right end of the curve (corresponding to η=1 and μ=0.35). Note that any member of the SM family has smaller SLPR than the binary filter and therefore produces a smaller bleaching effect. Note that the variation of SLPR with μ is close to linear. The smaller the value of μ is, the smaller SLPR is, and, consequently, the smaller the photobleaching effect. Also, with the smaller light throughput, the minimum value for SLPR is obtained with the unrealizable filter μ=1 η=1 (in fact the opaque screen). To deal with a realistic filter for our calculations, we select an intermediate SM filter corresponding to the pair μ=0.20, η=85. If we define the undesired bleaching as the one produced by the sidelobes, we find that the amount of undesired bleaching produced by the selected SM filter (SLPR =0.025) is 1.5 times smaller tha the one produced by the binary mask (SLPR=0.037). As it can be seen in Fig. 7, where we have added the curves corresponding to the selected SM filter, the OTF of the SM filter is superior to the one of the circular over the 63% of the spatial spectral range and to the one of the annular apertures over all the frequency range. So, we can conclude that the SM filters provide an effective improvement in spatial resolution.

5 Conclusions

We have shown that by the combined use of radially polarized illumination and SM filtering, one can obtain a tighter focal spot in which the sidelobes have been importantly reduced. The depolarization effect, inherent in high-aperture focused linearly polarized beams, has been avoided by means of incident radial polarization, and the reduction of sidelobes' strength permits the achievement of an effective superresolving effect, which can be very useful in scanning microscopy architectures. Our method improves the results obtained with annular filters because the sidelobes have been minimized by nearly a factor 1.5.

Acknowledgments

This work was funded by the Plan Nacional I+D+I (Grant No. DPI2003-04698), Ministerio de Ciencia y Tecnología, Spain. We also acknowledge the support from the Generalitat Valenciana (Grant No. IMCITA/2005/14), Spain.

References

1. E. Abbe, "Beiträge zur theorie des mikroskops und der mikroskopischen, Wahrnehmung," *Arch. Mikrosc. Anat. Entwicklungsmech.* **9**, 413–468 (1873).
2. T. R. M. Sales, "Smallest focal spot," *Phys. Rev. Lett.* **81**, 3844–3847 (1998).
3. C. J. R. Sheppard and A. Choudhury, "Annular pupils, radial polarization, and superresolution," *Appl. Opt.* **43**, 4322–4327 (2004).
4. M. Mansuripur, "Distribution of light at and near the focus of high-numerical-aperture objectives," *J. Opt. Soc. Am. A* **3**, 2086–2092 (1986).
5. K. Bahlmann and S. W. Hell, "Depolarization by high aperture focusing," *Appl. Phys. Lett.* **77**, 612–614 (2000).
6. I. J. Cooper, M. Roy, and C. J. R. Sheppard, "Focusing of pseudoradial polarized beams," *Opt. Express* **13**, 1066–1071 (2005).
7. O. Haeberlé, *Opt. Commun.* **235**, 1–3 (2004).
8. S. S. Sherif and P. Torok, *J. Mod. Opt.* **51**, 2007–2019 (2004).
9. J. W. M. Chon, X. Gan, and M. Gu, "Splitting of the focal spot of a high numerical-aperture objective in free space," *Appl. Phys. Lett.* **81**, 1576 (2002).
10. R. Dorn, S. Quabis, and G. Leuchs, "Sharper focus for a radially polarized light beam," *Phys. Rev. Lett.* **91**, 233901 (2003).
11. B. Richards and E. Wolf, *Proc. R. Soc. London, Ser. A* **253**, 368–379 (1959).
12. W. Denk, J. H. Strickler, and W. W. Webb, "Two-photon laser scanning flourescence microscopy," *Science* **248**, 73–76 (1990).
13. C. Ibáñez-López, G. Saavedra, G. Boyer, and M. Martínez-Corral, "Quasi-isotropic 3-D resolution in two-photon scanning microscopy," *Opt. Express* **13**, 6168–6174 (2005).
14. M. Martínez-Corral, C. Ibáñez-López, G. Saavedra, and M. T. Caballero, "Axial gain resolution in optical sectioning flourescence microscopy by shaded-ring filters," *Opt. Express* **11**, 1740–1745 (2003).
15. C. J. R. Sheppard, *Optik (Jena)* **99**, 32–34 (1995).

María Teresa Caballero received her BSc degree in optometry from the University of Alicante in 1996, and her BSc and MSc degrees in physics from the University of Valencia in 2000 and 2002, respectively. She is currently associate professor of optics at the University of Alicante. Since 2000, she has been working with the "3D Diffraction and Imaging Group" in the Optics Department, University of Valencia, Spain. Her research interest includes focusing properties of light and point-spread-function engineering in 3D microscopy. She has published more than 10 technical articles in major journals on these topics.

Cristina Ibáñez-López: Biography and photograph not available.

Manuel Martínez-Corral received his MSc and PhD degrees in physics from the University of Valencia in 1988 and 1993, respectively. He is currently associate professor of optics at the same university. Since 1999, he has led the 3D Diffraction and Imaging Group in the Optics Department. His research interest includes focusing properties of light, point-spread-function engineering in 3D microscopy, and 3D imaging acquisition and display. He has published more than 50 technical articles in major journals on these topics. He has published over 60 conference proceedings including over 10 invited presentations.